Fabrication of Anti-Counterfeiting Films by Dyeing Nanofibrillated cellulose (NFC) with Berberine

Mohammadreza Biabani [a], Mohammad Azadfallah [b,*] Soheila Izadyar [b] Morteza Sasani Ghamsari [c] and Sabrine Tavakoli Mohseni [d]

Incorporation of planchettes and use of films that are capable of taking part in color-forming reactions are the common methods in fabricating security paper documents. In this paper, novel nanofibrillated cellulose (NFC)-based films with high performance in optical properties were developed for use in anti-counterfeiting applications. To enhance dyeability of NFC with eco-friendly cationic berberine, functional modification was carried out by *in-situ* polymerization along with grafting approach with acrylic acid (AA-g-NFC). The achievement of grafting was demonstrated with determination of grafting percentage and further characterized by Fourier transform infrared spectroscopy. Tensile strength impairment of AA-g-NFC films, which was accompanied with alteration of crystallinity and partially changing the structure of cellulose I to cellulose II, was demonstrated by X-ray diffraction analysis. The variations of dyeing reaction time and temperature altered color strength of NFC due to different adsorption amounts of berberine. It can be concluded that exhibition of appropriate appearance characteristics, such as color, transparency, and color strength, render the berberine-dyed NFC films as a novel anti-counterfeiting element for applications such as security paper documents.

DOI: 10.15376/biores.21.2.3101-3114

Keywords: Cellulose nanofibril; Berberine; Grafting; Film; Anti-counterfeiting

Contact information: a: Wood and Paper Science and Technology Department, University of Tehran; b: Wood and Paper Science and Technology Department, University College of Agriculture and Natural Resources, University of Tehran; c: Photonics and Quantum Technologies Research School, Nuclear Science and Technology Research Institute, 11155-3486, Tehran, Iran; d: Head of Quality Control and Assurance of Securities Paper Production Factory, Takab, Iran;
** Corresponding author: adfallah@ut.ac.ir*

INTRODUCTION

Security paper is achieved by the addition of certain products into the paper structure during its manufacturing process (van Renesse 1997). Effective anti-counterfeiting techniques are often multilayered technologies consisting of features that are both overt (readily visible to the naked eye) or covert (undetectable without the use of special equipment and/or chemicals) features. Paper products can be protected against counterfeiting by creating watermarks, using a variety of special security fibers, yarns, reactive chemicals, volume holograms, and planchettes (Mercer 2002).

The planchettes are small elements incorporated into paper during the manufacturing process. They are usually embedded within the paper's surface fibers, providing specific functionality (see Fig. 1-a and b). For instance, these may consist of cellulose discs (1.25 mm in diameter) with certain attributes or transparent pigments in the

form of a thin film, which are not changed when they are added to the structure of the paper. The planchettes can be visible, as in the case of Canadian banknotes, or invisible as iridescent, as in the case of the new Dutch 100- and 1000-guilder banknotes as security features. There are several other countries, such as Mexico, for which planchettes are now included in the currency (van Renesse 1997; Soon and Manning 2019).

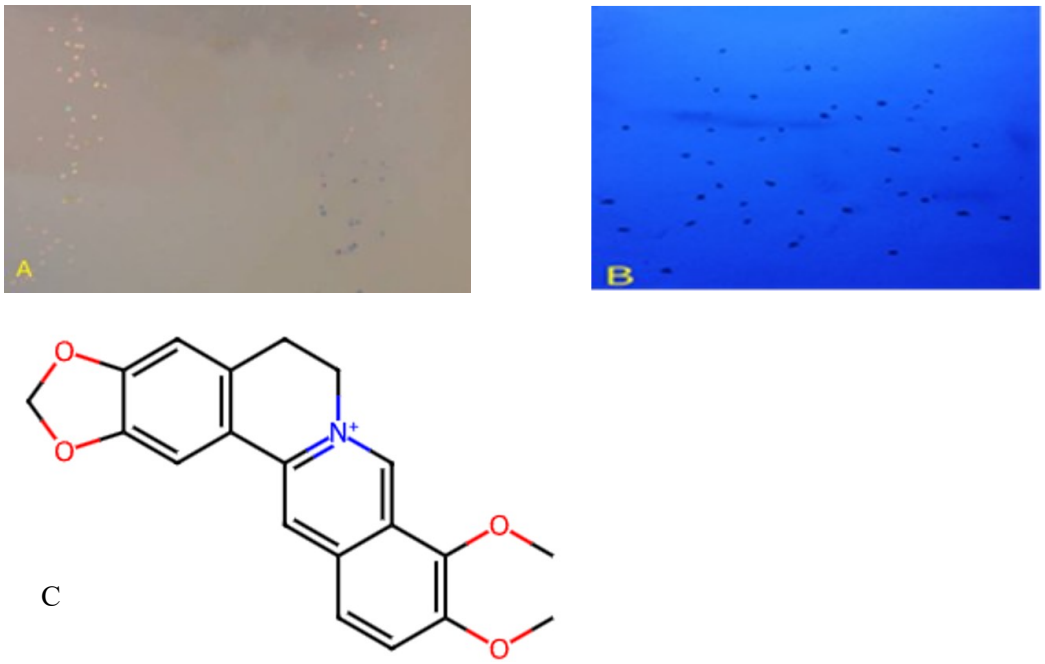

Fig. 1. (a) planchettes on surface of paper under visible/day light, (b) planchettes on surface of paper under UV-light, (c) chemical structure of berberine

The visible cellulosic discs with fluorescent or non-fluorescent properties (Bozhkova *et al.* 2017) can be colored with different materials, such as lanthanides (Hu *et al.* 2020), as well as by ordinary organic matters/dyes/pigments to render variety of colors (Jeon *et al*. 2015). However, despite their advantages, these materials have inherent drawbacks. Multi-step synthesis routes are time-intensive, require expensive precursors, and are associated with low photo/thermal stability and significant toxicity (Muthamma *et al.* 2021). While synthetic dyes including direct, vat, sulfur, azoic, and reactive dyes, offer convenience in fiber dyeing, growing concerns about the environmental impact and potential health risks associated with these chemicals have led to a surge in interest and spurred a significant shift towards natural dyes (Haji 2013). Natural dyes can be extracted from a vast array of plants, and some of them, such as berberine (Fig. 1-c), besides being an environmentally friendly product, have many advantages, such as fluorescence property with the absorption and emission maxima between 421 to 431 nm and 514 to 555 nm, as well as antimicrobial effects (Liu *et al.* 2019).

Cellulosic fibers are good candidate to be colored with natural dyes, but there are several problems associated with their use, including low affinity and poor fastness to cellulosic fibers (Kamel *et al.* 2009). In recent years, due to its exceptional properties, nanofibrillated cellulose (NFC) has become a focal point in materials science (Sharma and Varma 2017; Li and Hu 2019). Researchers are particularly interested in its potential

applications in enhancing security features (Li and Hu 2019; He *et al.* 2020; Cheng *et al.* 2021). Although NFC inherently contains some carboxyl groups, and conventional oxidation or carboxymethylation processes are often employed to enhance the anionic character, such approaches may reduce the crystallinity of NFC and deteriorate its physical properties (Kumar *et al.* 2014; Wohlhauser *et al.* 2018).

In this study, acrylic acid (AA) was selected as a grafting monomer for cellulose nanofibers. The primary goal was to maximize the number of binding sites for the cationic berberine dye. While established modification methods like carboxymethylation adds a monolayer of anionic groups, grafting poly(acrylic acid) creates a dense, 3D brush of carboxylic acid groups on the NFC surface and improves the hydrophilicity and electrostatic interactions of the nanofibers, thereby enhancing their compatibility with cationic molecules of berberine dye. This modification provides superior optical performance, which is a key requirement for the anti-counterfeiting applications of the prepared films.

EXPERIMENTAL

Materials

Berberine chloride hydrate (Natural Yellow18, > 98% purity), acrylic acid (AA), and potassium persulfate (KPS) were supplied from Sigma Aldrich (St. Louis, MO, USA) as Laboratory grade. Nanofibrillated cellulose gel (NFC) (1.6 g/100 g wet basis) was provided by Nano Novin Polymer Corporation (Iran).

This gel, produced from bleached kraft pulp using a chemo-mechanical method, has an approximate pH of 7 and a purity of over 99.9%. Its structure is characterized by the formula $(C_6H_{10}O_5)_n$, a molar mass of 162 g/mol, and a degree of polymerization between 800 and 1500. In terms of physical properties, this material has an aspect ratio of 100 to 350, and a crystallite size of 4 to 6 nm. The diameter of its nanofibers is also between 20 to 50 nm. This gel is dissolved in deionized water, and 0.1% methanol is used as a preservative to enhance its thermal stability up to approximately 260 °C.

Grafting Procedure

The polymerization of AA was conducted in an aqueous medium through a radical polymerization mechanism, with KPS serving as the initiating agent. The grafting reaction was performed in a flask under controlled conditions. The potassium persulfate (1.0% based on AA weight, w/w) was dissolved in distilled water. The required amount of acrylic acid (based on raw material weight W/W) was then added, and the mixture was stirred for various durations (30 and 60 minutes) while keeping the flask in a water bath. The specific stirring times and their corresponding results are presented in Table 2.

After the reaction was complete, to remove unreacted acrylic acid and homopolymers adhering to the surface, and to achieve a constant weight, the grafted nanocellulose samples were centrifuged three times at 8000 rpm for 10 minutes. Each time, the material was resuspended uniformly in deionized water. By centrifuging the samples multiple times at high speed, unreacted monomers and homopolymers adhered to the nanofiber surfaces were effectively removed from the grafted NFC without causing significant loss of material or altering the fiber morphology. This approach has also been reported as a purification protocol in NFC grafting studies (Wang et al., 2018).
The grafting percentage was calculated according to the following Eq. (1),

$$\text{Grafting \%} = [(W_1\text{-}W_2)/W_1] \times 100 \quad (1)$$

where W_1 and W_2 are the weights (g) of grafted NFC and pure NFC, respectively.

Dyeing Method and Preparation of Films

The acrylic acid grafted nanofibrillated cellulose (AA-g-NFC) were dyed with berberine (2% oven dry weight of fiber, owf) at various temperatures of 30, 45, and 60 ºC and reaction time of 30 and 45 min. The liquor to NFC ratio was 100:1. At the end of dyeing period, the samples were removed and rinsed thoroughly by centrifugation.

To prepare films, the berberine-dyed AA-g-NFC was homogenized for 5 min and degassed using an ultrasonic system (SONICA, Milano, Italy). A 50 mL of suspension was then uniformly cast onto an 80 mm diameter polystyrene petri dish and dried at room conditions for 2 days.

Characterization of Modified NFC

Fourier Transform-infrared (FTIR) measurements were performed using a Bruker Tensor 27 FTIR Spectrometer (Bruker Inc., Bremen, Germany). Spectra were collected in the range of 4000 to 400 cm^{-1} with an average of 45 scans and a resolution of 4 cm^{-1}. The spectra were normalized with min-max method to the range [0,1] using Origin Pro 2024.

Philips X'Pert PW 3040/60 (Almelo, Netherlands) diffractometer was used to record X-ray diffraction patterns of untreated and modified NFC samples. Diffraction patterns were recorded from 2θ =10 to 60° using CuKa radiation at 45 KV and 40 mA. The crystallinity index, CrI, was calculated according to Eq. 2,

$$\text{Cr I} = (I_{oo2} - I_{am})/I_{002} \quad (2)$$

where I_{002} is the overall intensity of the peak at 2θ = 22° and I_{am} is the intensity of the baseline at 2θ = 18°, *i.e.*, the diffraction intensity of the amorphous region.

Optical and Mechanical Properties

The optical properties of the films were characterized through the measurement of color strength, color parameters, and light transmittance. A Color-Eye 3100 spectrophotometer (Gretag Macbeth, USA) was used to measure the reflectance of the samples, and the color strength (K/S) of each dyed sample was calculated using the Kubelka–Munk equation,

$$K/S = (1-R)^2/2R \quad (3)$$

where R is the reflectivity (%), K is the absorption coefficient, and S is the light scattering coefficient.

For color measurements, the L^*, a^*, and b^* parameters of the films were determined using a Konica Minolta Lab CR-10 colorimeter. The total color difference (ΔE) was calculated using the following equation:

$$\Delta E^* = \sqrt{(\Delta l^*)^2 + (\Delta a^*)^2 + (\Delta b^*)^2} \quad (4)$$

Finally, the light transmittance of the films was measured from 360 to 750 nm using a UV-Vis spectrophotometer (Agilent Cary 5000, Santa Clara, CA, USA). Both berberine-stained and pristine NFC films were cut into 40 mm x 10 mm rectangles and analyzed in a quartz cuvette.

The NFC specimens with dimensions of 10 × 50 mm^2 were prepared and conditioned at 23 ºC and 50% relative humidity (RH). The tensile strength and elongation at break were then measured using a Santam test machine at 3 mm/min strain rate.

RESULTS AND DISCUSSION

Graft Polymerization of Acrylic Acid onto NFC

Free radical polymerization (FRP) is an effective technique in surface modification of fiber that is widely used in grafting vinyl polymers onto cellulose. The polymerization is initiated by thermal activation of potassium persulfate (KPS) as a common initiator to generate relatively stable free radical species in aqueous medium for initiation followed by formation a reactive radical on the NFC surface *via* hydrogen abstraction. The polymerization is then propagated by adding monomers to the propagating chain (Fig. 2).

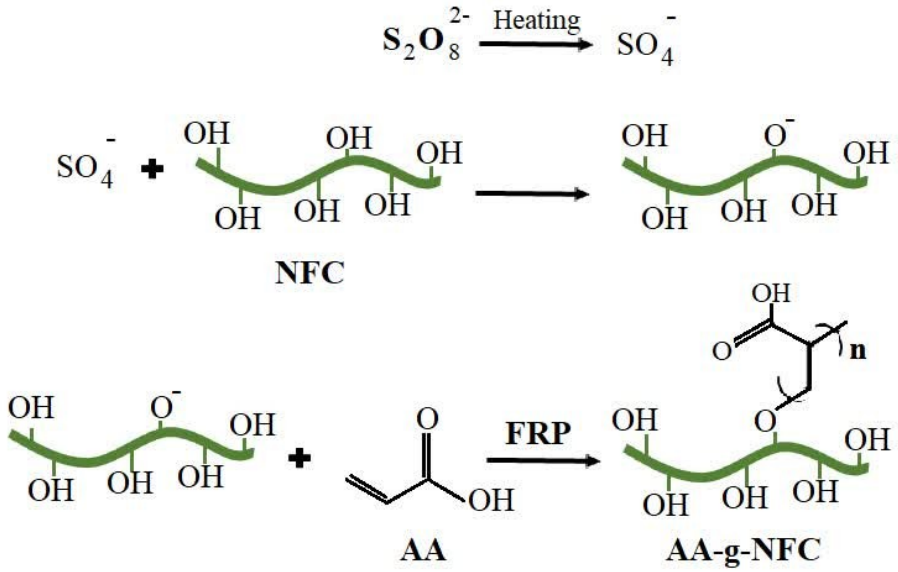

Fig. 2. Schematic of nanofibrillated cellulose modification with acrylic acid grafting

The resulting modified NFC with the anionic agent (acrylic acid) as a vinyl polymer with the formula CH_2 = CHCOOH were studied by FTIR spectroscopy in terms of developing bonding active sites for cationic dye. As shown in Fig. 3, a peak was clearly apparent around 1720 cm^{-1}, which is related to the tensile vibration of C=O in acrylic acid. This indicates the bonding of poly(acrylic acid) on the backbone of the nanocellulose. The grafted polymer provides a mechanism for better binding of cationic dye molecules to the junctions of the sites. In addition to C=O stretching of COOH, the changes of O-H and C-O-C stretching of cellulose can also reflect the hydrogen bonding between cellulose and PAA.

According to the treatments performed in different reaction conditions (see Tables 1 and 2), including various ratios of monomer to NFC (10:1, 8:1, 5:1, 3:1, 2:1), time (60 and 30 min) and temperature of 60 and 45 °C, observations show that the bonding performance increased with increasing the reaction time from 30 min to 60 min. Table 1 shows that at the temperature of 60 °C for 60 min and in the ratio of 10:1 the highest

efficiency was achieved in terms of percentage of grafting.

One of the positive research results from this study, compared to the study by Loria-Bastarrachea *et al*. (2002) on acrylic acid bonding to micro-celluloses is the maximum bond yield, which was more than twice as high. This may be attributed to the high specific surface of NFC in the grafting reaction. The distinctive properties of nanocellulose, as opposed to micro or macrocellulose, can be attributed to its nanoscale size, leading to a significantly higher specific surface area. This, coupled with the abundance of free hydroxyl groups on its surface, renders it highly reactive and provides ample opportunities for surface chemical modifications (Zhu and Lin 2019; Shoseyov *et al.* 2019).

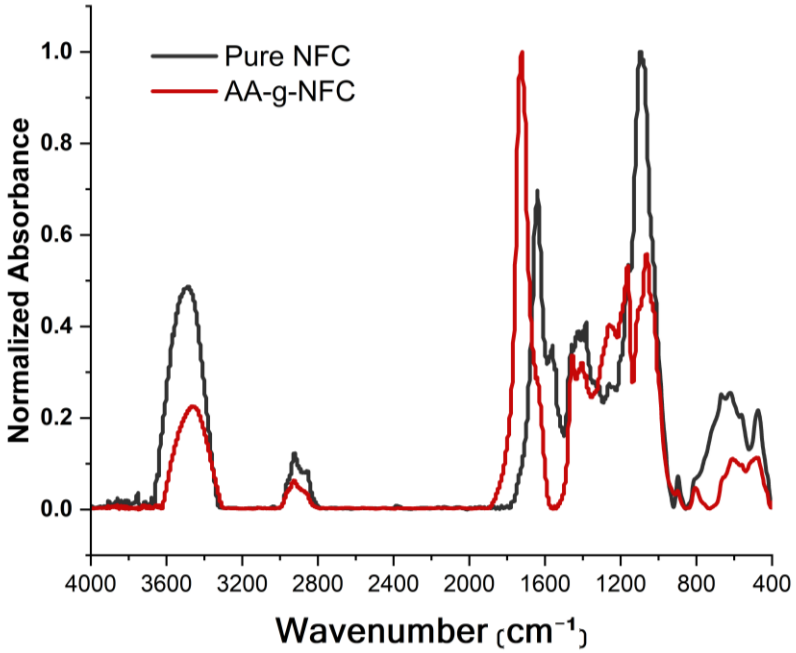

Fig. 3. Normalized FTIR spectra of pure NFC and AA-g-NFC

Table 1. Effect of AA Monomer to NFC Ratio on Grafting Percentage

Treatment	Monomer: NFC Ratio (w/w)	Temperature (°C)		Time (min)	Grafting Percentage
A	10:1	60		60	25
B	8:1	60		60	24
C	5:1	60		60	21.9
D	3:1	60		60	15.6
E	2:1	60		60	6.2

Table 2. Effect of Grafting Conditions on Grafting Percentage

Treatment	Monomer: NFC Ratio (w/w)	Temperature (°C)	Time (min)	Grafting Percentage
A	10: 1	60	60	25
F	10: 1	60	30	18.8
G	10: 1	45	60	12.5
H	10: 1	45	30	9.4

Tensile Strength

A clear difference of mechanical behavior between grafted NFC and pure NFC films was evident (see Table 3). The AA grafting on cellulose resulted in an increase in elongation at break while decreasing tensile strength and modulus of elasticity. The latter may be attributed to degradation of the crystalline structure of the cellulose due to incorporation of acrylic acid, which was well demonstrated with XRD analyses. This phenomenon can be explained by a synergy due to the plasticizing effect of the poly(acrylic acid) side-chains, disrupting the close packing of the NFC during film formation.

It is also believed that in most polymers, high modulus causes a decrease in elongation and is disadvantageous for flexibility. In addition, flexibility of side chain PAA may contribute to increase elongation of modified NFC film under tensile loading (Yang *et al.* 2012).

Table 3. Mechanical Strength of Pure NFC and AA-g-NFC Films

	Elongation at Break (%)	Tensile Strength (MPa)	MOE (GPa)
NFC film	0.42	20.12	3.44
AA-g-NFC film	0.77	14.39	1.65

XRD Analyses

As can be seen from Fig. 4, the XRD patterns of pure NFC, as a raw material, displayed relatively sharp diffraction peaks at 2θ = 16.3°, 22.4°, and 34.1°, which correspond to the characteristics of the (101′), (002), and (040) crystalline planes positions of the cellulose I structure, respectively. The introduction of PAA to NFC resulted in a dramatic alteration in their XRD patterns. The appearance of a single, broad diffraction peak between 10 and 20° is a signature of the amorphous domains induced by PAA. This showed that grafting resulted in decreasing the peak intensity of AA-grafted NFC sample.

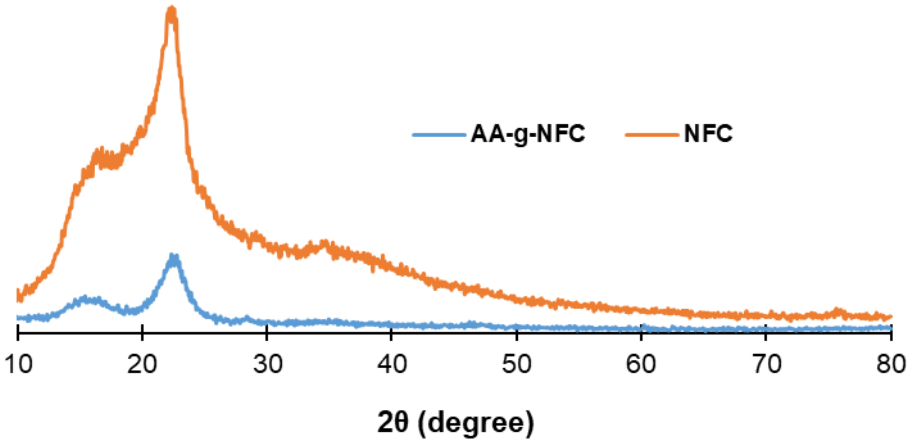

Fig. 4. XRD patterns of NFC and AA-g-NFC

The decrease of XRD peak intensity and peak broadening of AA-g-NFC pattern may be attributed to increase in amorphous phase as a result of alkaline conditions of the grafting method (Dima *et al.* 2017). Furthermore, AA grafting appears to disrupt intramolecular hydrogen bonds, leading to a rearrangement of cellulose molecules into a less ordered state, which is typical of amorphous polymers. In other words, the grafting

reaction induced a structural transformation from the crystalline cellulose I to a relatively amorphous state, commonly associated with cellulose II. The CrI of 31% for grafted NFC demonstrates well this alteration in cellulose structure compared to pure NFC with CrI of 43%. In a similar study, it was reported that the interpenetration of poly(acrylic acid) significantly altered the crystalline structure of cellulose (Shahzamani *et al.* 2020). Consequently, the high amorphous state (Iwamoto *et al.* 2018; Zhao *et al.* 2019), large specific surface area, and morphology of AA-g-NFC allow facile access to anionic sites by cationic berberine dye, making it ideal as an overt element for rendering an anti-counterfeiting feature as manifested itself by enhancement of color strength.

Color Strength

The *K*/*S* values of the berberine-dyed film samples are presented in Fig. 5. As expected, the transparent films made of AA-g-NFC as a control sample exhibited negligible color strength. However, the maximum value of *K*/*S* was obtained for samples dyed at 60 °C for 45 min at 430 nm (see Fig. 5-a). The high *K*/*S* value at 430 nm indicates strong absorption by berberine relative to scattering. According to the Kubelka-Munk model (Eq. 3), $K/S \approx (1-R)^2/2R$, where R is reflectivity. For highly transparent films with minimal scattering ($S \rightarrow 0$), the *K*/*S* ratio effectively represents the absorption coefficient (K) of the dye. Thus, the maximum *K*/*S* observed at 60 °C for 45 min (Fig. 5a) corresponds to the highest concentration of berberine adsorbed onto the AA-g-NFC, confirming successful dye immobilization.

In the other treatment, in which the dyeing process lasted for 30 min, the maximum value of *K*/*S* also was associated with the temperature of 60 °C (Fig. 5-b). Temperature had an obvious effect on the dyeing system. As the concentration of dye molecules in the dye bath decreases due to the absorption process, the driving force for further dye uptake is maintained. The specific mechanism of dye absorption, however, depends on the nature of the dye, the fiber, and the dyeing conditions. Because the absorption of berberine on the NFC increases continuously with increasing temperature, the internal structure of cellulose also swells under temperature impacts, which facilitates the penetration of dye compounds into its structure.

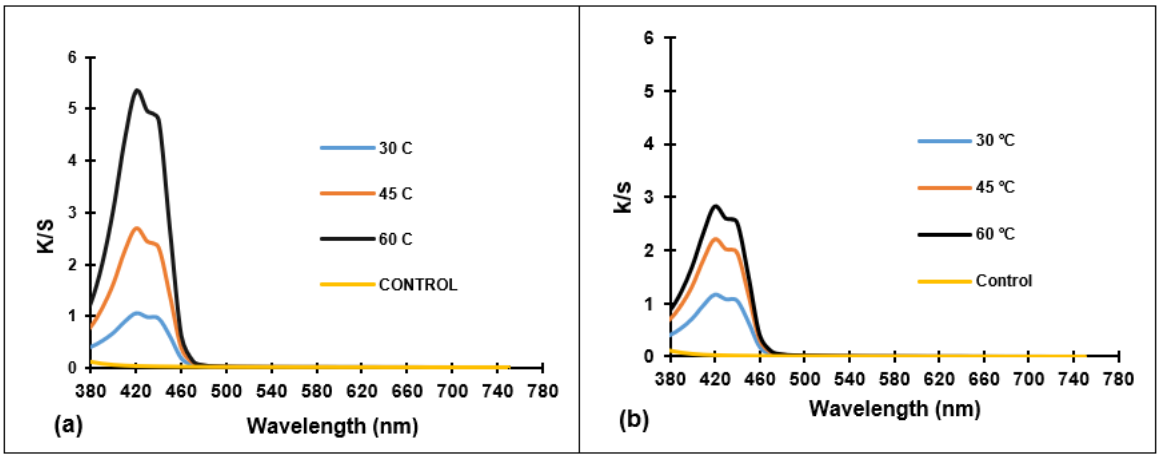

Fig. 5. Effect of temperature variations in dyeing process of NFC with berberine on color strength (K/S) at a) reaction time of 45 min and b) reaction time of 30 min

It can be observed that time was also an effective variable in dyeing so that the adsorption of berberine on cellulose nanofibers increased with increased time of dyeing process. In addition, the observed variations in *K*/*S* values under different dyeing conditions can serve as unique optical fingerprints of the films, which are highly relevant for anti-counterfeiting applications, since reproducing such specific reflectance-based color strengths is technically challenging.

Color Measurements

As shown in Table 4, color parameters *L**, *a**, and *b** were employed to assess how different dyeing variables could influence the appearance characteristics of the NFC films. The parameters *a** and *L**, which represent the redness and whiteness of the dyed samples dropped with rising the reaction temperature of berberine with NFC substrate. In contrast, *b**, which represents the yellowing component of colors for the stained film, increased with reaction temperature. This yellow shadow is attributed to the yellow nature of berberine dye. However, all samples experienced considerable total color changes (Δ*E**) with increasing dyeing temperature. The results were in line with color strength and grafting percentage results. These significant differences in colorimetric parameters (*L**, *a**, *b**, and Δ*E**) may further contribute to the anti-counterfeiting potential of the dyed films, as subtle shifts in color coordinates provide distinctive visual signatures that are difficult to imitate.

Table 4. The CIELab Coordinates and Color Difference of NFC Films Dyed with Berberine at Various Conditions of Time and Temperature

	Temperature	*L**	*a**	*b**	Δ*E**
Control	-	90.37	0.23	0.04	-
45 min	30°C	90.82	6.89	30.20	30.88
	45°C	90.25	7.77	41.30	42.00
	60°C	89.93	8.02	50.04	50.60
30 min	30°C	90.00	7.05	39.09	39.63
	45°C	87.54	7.66	44.49	45.15
	60°C	86.44	7.67	50.10	50.76

Transmittance

Selective reflection or the passage of light at a given wavelength for planchettes is widely addressed as a security feature. Furthermore, transparency is a critical characteristic of NFC-based films, particularly for applications where visual appeal and consumer acceptance are paramount. To achieve transparency, the fibers must be efficiently packed within the films, and porosity must be minimized (Jacucci *et al.* 2021). The optical properties of pure NFC and dyed NFC films were assessed by measuring the light transmittance at the region of 360 to 750 nm (Fig. 6). Dyeing NFC with berberine at different conditions show no noticeable difference in transmittance at visible range of about 460 to 760 nm in comparison with pure-NFC film. In addition, the retention of transparency of the dyed NFC films proposes good compatibility of the AA-g-NFC with berberine. Transmittance values of all samples measured within the visible wavelengths of 460 to 760 nm were approximately 90%.

As shown in Fig. 7, the photographs taken from pure- and dyed samples over a printed text also confirms the acceptable obtained transparency of films to be used as a novel anti-counterfeit material. However, reaction of the berberine with NFC impaired the

transmittance of the dyed films in the range of 360 to 460 nm, but the control sample retained its transparency. Therefore, the combination of high transparency in the visible range with selective UV-blocking behavior offers an additional layer of security functionality. Such unique optical features (transparency retention, selective reflection, and UV absorption by berberine molecules) can be directly associated with the anti-counterfeiting potential of these films, in agreement with previous studies on cellulose-based security materials (Jacucci *et al*. 2021; Ma *et al*. 2021; Ahmad *et al.* 2021). As can be observed, the UV-blocking property was improved by increasing berberine adsorption through elevating temperature relative to the influence of dyeing duration, which can be mainly attributed to the ultraviolet absorption by the benzene rings and a carbonyl group (Ma *et al.* 2021). The peak absorption was observed at a wavelength of around *ca.* 440 nm. This absorption was attributed to the n–π* electronic transition originating from the surface groups and aligned with findings from previous studies (Ahmad *et al.* 2021). It is evident that the presence of multiple unsaturated bonds in the structure of the berberine molecule is responsible for the absorption of ultraviolet/visible radiation (Bitencourt *et al.* 2014; Hu *et al.* 2020).

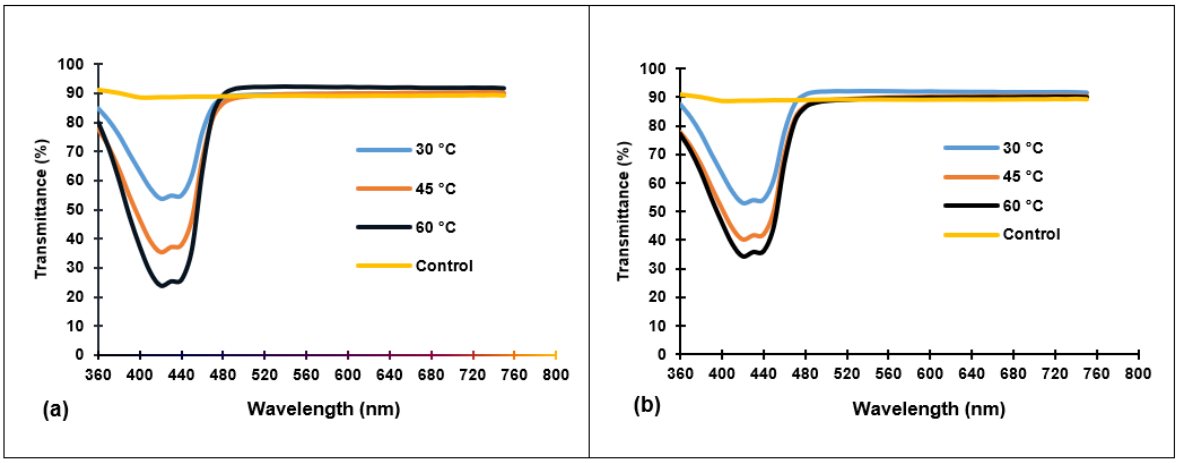

Fig. 6. Transmittance of NFC films dyed under temperature of 30 ºC, 45 ºC, and 60 ºC at a) reaction time of 45 min and b) reaction time of 30 min

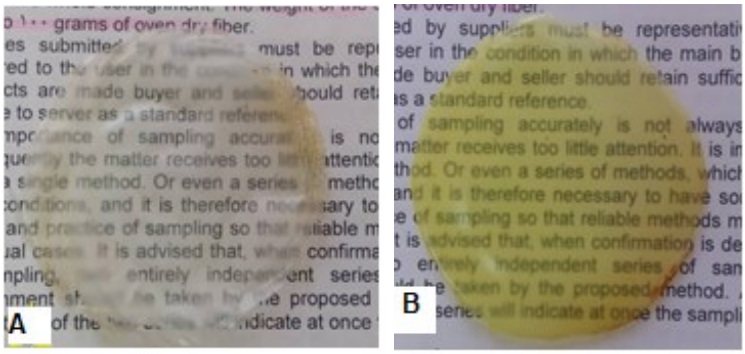

Fig. 7. Photographs of pure NFC film (A) and berberine-dyed NFC film (B) over a printed text

CONCLUSIONS

The authors made an effort to fabricate non-fluorescent nanocellulose planchettes with the aim of reducing environmental pollution and safety problems caused by artificial colors. These thin films (planchettes) with various changes are based on dyeing with natural berberine dye protect against counterfeits based on printing and the main threats for some applications.

1. Temperature, acrylic acid (AA) concentration, and reaction time are key factors affecting the grafting of acrylic acid onto nanofibrillated cellulose (NFC).
2. Ionic interactions between berberine and the acrylic acid-modified nanofibrillated cellulose (NFC) were responsible for the enhanced color strength of the colored films, suggesting successful immobilization of the dye onto the modified fiber.
3. The acrylic acid-grafted nanofibrillated cellulose (AA-g-NFC) due to its good compatibility with berberine allowed the dyed films to maintain their transparency within the visible wavelengths of 460 to 760 nm.
4. Berberin-dyed NFC film can be designed to supplement existing safety features used in security paper and printing technology. However, they may be designed with berberine fluorescence enhancers or fluorescent emitters element if needed.
5. While the current grafting and dyeing approach demonstrates a successful proof-of-concept for creating distinctive optical features, the authors acknowledge that scaling such a multi-step nanocellulose modification process presents economic and practical challenges for high-volume security paper production. Future work will focus on simplifying the chemistry and integrating the functionalized NFC into papermaking furnish at lower addition levels to improve cost-effectiveness, as suggested by Hubbe (2020).

REFERENCES CITED

Ahmad, M. A., Aslam, S., Mustafa, F., and Arshad, U. (2021). "Synergistic antibacterial activity of surfactant free Ag–GO nanocomposites," *Scientific Reports* 11(1), article 196. https://doi.org/10.1038/s41598-020-80013-w

Bitencourt, C. M., Fávaro-Trindade, C. S., Sobral, P. D. A., and Carvalho, R. A. (2014). "Gelatin-based films additivated with curcuma ethanol extract: Antioxidant activity and physical properties of films," *Food Hydrocolloids* 40, 145-152. https://doi.org/10.1016/j.foodhyd.2014.02.014

Bozhkova, T., Spiridonov, I., and Shterev, K. (2017). "Overview of security printing types and trends in its future development," *Bulgarian Chemical Communications* 49(Special Issue L), 195-201.

Cheng, H., Wei, X., Qiu, H., Wang, W., Su, W., and Zheng, Y. (2021). "Chemically stable fluorescent anti-counterfeiting labels achieved by UV-induced photolysis of nanocellulose," *RSC Advances* 11(30), 18381-18386. https://doi.org/110.1039/D1RA02089G

Chen, Y., Li, Q., Li, Y., Zhang, Q., Huang, J., Wu, Q., and Wang, S. (2020). "Fabrication of cellulose nanocrystal-g-poly(acrylic acid-co-acrylamide) aerogels for efficient Pb(II) removal," *Polymers* 12(2), 333. https://doi.org/10.3390/polym12020333

Chu, L., Zhang, X., Niu, W., Wu, S., Ma, W., Tang, B., and Zhang, S. (2019). "Hollow silica opals/cellulose acetate nanocomposite films with structural colors for anti-counterfeiting of banknotes," *Journal of Materials Chemistry C* 7(24), 7411-7417. https://doi.org/https://doi.org/10.1039/C9TC01992H

Dima, S. O., Panaitescu, D. M., Orban, C., Ghiurea, M., Doncea, S. M., Fierascu, R. C., Nistor, C. L., Alexandrescu, E., Nicolae, C. A., Trică, B., *et al.* (2017). "Bacterial nanocellulose from side-streams of kombucha beverages production: Preparation and physical-chemical properties," *Polym.* 9(8), article 374. https://doi.org/10.3390/polym9080374

Haji, A. (2013). "Eco-friendly dyeing and antibacterial treatment of cotton," *Cellulose Chemistry and Technology* 47(3-4), 303-308.

He, Y., Du, E., Zhou, X., Zhou, J., He, Y., Ye, Y., Wang, J., Tang, B., and Wang, X. (2020). "Wet-spinning of fluorescent fibers based on gold nanoclusters-loaded alginate for sensing of heavy metal ions and anti-counterfeiting," *Spectrochimica Acta Part A: Molecular and Biomolecular Spectroscopy* 230, article 118031. https://doi.org/10.1016/j.saa.2020.118031

Hu, W., Li, T., Liu, X., Dastan, D., Ji, K., and Zhao, P. (2020). "1550 nm pumped upconversion chromaticity modulation in Er3+ doped double perovskite LiYMgWO6 for anti-counterfeiting," *Journal of Alloys and Compounds* 818, article 152933. https://doi.org/10.1016/j.jallcom.2019.152933

Hu, X., Yuan, L., Han, L., Li, S., and Zhou, W. (2020). "The preparation, characterization, anti-ultraviolet and antimicrobial activity of gelatin film incorporated with berberine-HP-β-CD," *Colloids and Surfaces A: Physicochemical and Engineering Aspects* 586, article 124273.

Hubbe, M. A. (2020). "Security papers: Trust but verify," in: *Make Paper Products Stand Out. Strategic Use of Wet End Chemical Additives*, M. A. Hubbe and S. Rosencrance, S. (eds.) TAPPI Press, Atlanta, GA, Ch. 6, pp. 129-154

Iwamoto, M., Shimatai, A., Honda, M., and Matsukata, M. (2018). "Depolymerization of cellulose with superheated steam: Remarkable obstruction effects of sodium and high reactivity of crystalline cellulose," *ACS Sustainable Chemistry & Engineering* 6(5), 6570-6576. https://doi.org/10.1021/acssuschemeng.8b00375

Jacucci, G., Schertel, L., Zhang, Y., Yang, H., and Vignolini, S. (2021). "Light management with natural materials: From whiteness to transparency," *Advanced Materials* 33(28), article 2001215. https://doi.org/10.1002/adma.202001215

Jeon, S., Lee, J. P., and Kim, J. M. (2015). "*In situ* synthesis of stimulus-responsive luminescent organic materials using a reactive inkjet printing approach," *Journal of Materials Chemistry C* 3(12), 2732-2736. https://doi.org/10.1039/C5TC00334B

Kamel, M. M., Helmy, H. M., and El Hawary, N. S. (2009). "Some studies on dyeing properties of cotton fabrics with *Crocus sativus* (saffron flowers) using an ultrasonic method," *Journal of Natural Fibers* 6(2), 151-170. https://doi.org/10.1515/aut-2009-090105

Kumar, A., Negi, Y. S., Choudhary, V., and Bhardwaj, N. K. (2014). "Characterization of cellulose nanocrystals produced by acid-hydrolysis from sugarcane bagasse as agro-waste," *Journal of Materials Physics and Chemistry* 2(1), 1-8. https://doi.org/10.12691/jmpc-2-1-1

Li, X., and Hu, Y. (2019). "Luminescent films functionalized with cellulose nanofibrils/CdTe quantum dots for anti-counterfeiting applications," *Carbohydrate Polymers* 203, 167-175. https://doi.org/10.1016/j.carbpol.2018.09.028

Liu, J., Lin, X., and Liang, H. E. (2019). "Dyed fabrics modified *via* assembly with phytic acid/berberine for antibacterial, UV resistance, and self-cleaning applications," *Journal of Engineered Fibers and Fabrics* 14, article 1558925019888978. https://doi.org/10.1177/1558925019888978

Loría-Bastarrachea, M. I., Carrillo-Escalante, H. J., and Aguilar-Vega, M. J. (2002). "Grafting of poly (acrylic acid) onto cellulosic microfibers and continuous cellulose filaments and characterization," *Journal of Applied Polymer Science* 83(2), 386-393.

Ma, K., Zhe, T., Li, F., Zhang, Y., Yu, M., Li, R., and Wang, L. (2021). "Sustainable films containing AIE-active berberine-based nanoparticles: A promising antibacterial food packaging," *Food Hydrocolloids* 123, article 107147. https://doi.org/10.1016/j.foodhyd.2021.107147

Mercer, J. W. (2002). "Evaluation of optical security features in ID documents, currency, and stamps," in: *Proceedings of Optical Security and Counterfeit Deterrence Techniques IV* 4677, 323-332. https://doi.org/10.1117/12.462725

Muthamma, K., Sunil, D., Shetty, P., Kulkarni, S. D., Anand, P. J., and Kekuda, D. (2021). "Eco-friendly flexographic ink from fluorene-based Schiff base pigment for anti-counterfeiting and printed electronics applications," *Progress in Organic Coatings* 161, article 106463. https://doi.org/10.1016/j.porgcoat.2021.106463

Regula (2008). "Glossary of banknotes [cited 2016-03-03]," Available from: (http://www.regulaforensics.com), Accessed 03 March 2025.

Shahzamani, M., Taheri, S., Roghanizad, A., Naseri, N., and Dinari, M. (2020). "Preparation and characterization of hydrogel nanocomposite based on nanocellulose and acrylic acid in the presence of urea," *International Journal of Biological Macromolecules* 147, 187-193. https://doi.org/10.1016/j.ijbiomac.2020.01.038

Sharma, P. R., and Varma, A. J. (2017). "Functionalized cellulose nanofibers for advanced applications," *Carbohydrate Polymers* 173, 515-532. https://doi.org/10.1016/j.carbpol.2017.06.018

Shoseyov, O., Kam, D., Shalom, T. B., Shtein, Z., Vinkler, S., and Posen, Y. (2019). "Nanocellulose composite biomaterials in industry and medicine," in: *Extracellular Sugar-Based Biopolymers Matrices*, Springer, Cham, Switzerland, pp. 693-784. https://doi.org/10.1007/978-3-030-12919-4_17

Soon, J. M., and Manning, L. (2019). "Developing anti-counterfeiting measures: The role of smart packaging," *Food Research International* 123, 135-143. https://doi.org/10.1016/j.foodres.2019.04.049

van Renesse, R. L. (1997). "Paper based document security-A review," in: *European Conference on Security and Detection* ECOS 97, IET, London, UK, pp. 75-80. https://doi.org/10.1049/cp:19970425

Wang, Q., Yang, X., and Chen, J. (2018). "Grafting modification of cellulose nanofibers for functional materials," *Cellulose* 25, 3145-3164. https://doi.org/10.1007/s10570-018-1771-5

Wohlhauser, S., Delepierre, G., Labet, M., Morandi, G., Thielemans, W., Weder, C., and Zoppe, J. O. (2018). "Grafting polymers from cellulose nanocrystals: Synthesis, properties, and applications," *Macromolecules* 51(16), 6157-6189. https://doi.org/10.1021/acs.macromol.8b00733

Yang, J., Han, C. R., Duan, J. F., Ma, M. G., Zhang, X. M., Xu, F., Sun, R. C., and Xie, X. M. (2012). "Studies on the properties and formation mechanism of flexible nanocomposite hydrogels from cellulose nanocrystals and poly (acrylic acid)," *Journal of Materials Chemistry* 22(42), 22467-22480.

Ye, X., Wang, S., Zhou, P., Zhang, D., and Zhu, P. (2023). "Fluorescent cellulose nanocrystals/waterborne polyurethane nanocomposites for anti-counterfeiting applications," *Physical Chemistry Chemical Physics* 25(13), 9492-9499.

Zhao, J., Ding, L., Sui, X., Mao, Z., Xu, H., Zhong, Y., Zhang, L., Chen, Z., and Wang, B. (2019). "Bio-based polymer colorants from nonaqueous reactive dyeing of regenerated cellulose for plastics and textiles," *Carbohydrate Polymers* 206, 734-741. https://doi.org/10.1016/j.carbpol.2018.11.056

Zhu, G., and Lin, N. (2019). "Surface chemistry of nanocellulose," in: *Nanocellulose: from Fundamentals to Advanced Materials*, Wiley-VCH, Hoboken, NJ, USA, pp. 115-153. https://doi.org/10.1002/9783527807437.ch5

Article submitted: March 28, 2025; Peer review completed: Aug. 15, 2025; Revised version received: Aug. 28, 2025; Accepted: Feb. 4, 2026; Published: February 11, 2026.
DOI: 10.15376/biores.21.2.3101-3114